⌘ *Author's Choice*

Characterization and Structure of the *Aquifex aeolicus* Protein DUF752

A BACTERIAL tRNA-METHYLTRANSFERASE (MnmC2) FUNCTIONING WITHOUT THE USUALLY FUSED OXIDASE DOMAIN (MnmC1)*ˢ

Aya Kitamura[‡], **Madoka Nishimoto**[§], **Toru Sengoku**[§], **Rie Shibata**[§], **Gunilla Jäger**[¶], **Glenn R. Björk**[¶], **Henri Grosjean**[‖1], **Shigeyuki Yokoyama**[§**2], and **Yoshitaka Bessho**[‡§3]

From the [‡]RIKEN SPring-8 Center, Harima Institute, 1-1-1 Kouto, Sayo, Hyogo 679-5148, Japan, the [§]RIKEN Systems and Structural Biology Center, 1-7-22 Suehiro-cho, Tsurumi-ku, Yokohama, Kanagawa 230-0045, Japan, the [¶]Department of Molecular Biology, Umea University, S-90187 Umea, Sweden, the [‖]Centre de Génétique Moléculaire, UPR 3404, CNRS, Université Paris-Sud, FRC 3115, 1 Avenue de la Terrasse, 91190 Gif-sur-Yvette, France, and the [**]Laboratory of Structural Biology and Department of Biophysics and Biochemistry, Graduate School of Science, University of Tokyo, 7-3-1 Hongo, Bunkyo-ku, Tokyo 113-0033, Japan

Background: *Escherichia coli* encodes a bifunctional oxidase/methyltransferase catalyzing the final steps of methylaminomethyluridine (mnm^5U) formation in tRNA wobble positions.

Results: *Aquifex aeolicus* encodes only a monofunctional aminomethyluridine-dependent methyltransferase, lacking the oxidase domain.

Conclusion: An alternative pathway exists for mnm^5U biogenesis.

Significance: Information about how an organism modifies the wobble base of its tRNA is important for understanding the emergence of the genetic code.

Post-transcriptional modifications of the wobble uridine (U34) of tRNAs play a critical role in reading NNA/G codons belonging to split codon boxes. In a subset of *Escherichia coli* tRNA, this wobble uridine is modified to 5-methylaminomethyluridine (mnm^5U34) through sequential enzymatic reactions. Uridine 34 is first converted to 5-carboxymethylaminomethyluridine ($cmnm^5U34$) by the MnmE-MnmG enzyme complex. The $cmnm^5U34$ is further modified to mnm^5U by the bifunctional MnmC protein. In the first reaction, the FAD-dependent oxidase domain (MnmC1) converts $cmnm^5U$ into 5-aminomethyluridine (nm^5U34), and this reaction is immediately followed by the methylation of the free amino group into mnm^5U34 by the *S*-adenosylmethionine-dependent domain (MnmC2). *Aquifex aeolicus* lacks a bifunctional MnmC protein fusion and instead encodes the Rossmann-fold protein DUF752, which is homologous to the methyltransferase MnmC2 domain of *Escherichia coli* MnmC (26% identity). Here, we determined the crystal structure of the *A. aeolicus* DUF752 protein at 2.5 Å resolution, which revealed that it catalyzes the *S*-adenosylmethionine-dependent methylation of nm^5U *in vitro*, to form mnm^5U34 in tRNA. We also showed that naturally occurring tRNA from *A. aeolicus* contains the 5-mnm group attached to the C5 atom of U34. Taken together, these results support the recent proposal of an alternative MnmC1-independent shortcut pathway for producing mnm^5U34 in tRNAs.

Transfer RNAs (tRNAs) contain a wide variety of post-transcriptionally modified nucleosides. Among them, the wobble nucleoside at position 34 of the tRNA anticodon is the most diversely modified one identified so far in a naturally occurring cellular tRNA (1). The types of chemical adducts existing on the various atoms of nucleoside 34 strongly depend on the isoacceptor tRNA and the organism from which the nucleic acid originated (2, 3). For example, in *Escherichia coli* tRNA^Gln, tRNA^Lys, and tRNA^Glu, the wobble uridine 34 is hypermodified into a 5-methylaminomethyl-2-thiouridine (mnm^5s^2U),[4] whereas in tRNA^Arg and tRNA^Gly, only a 5-mnm group is found on the nonthiolated U34 (mnm^5U). In one of the two *E. coli* U34-containing tRNA^Leu molecules, the C5 atom of U34 is modified into a cmnm group, and its 2′-hydroxyl ribose is methylated into Um, leading to the doubly hypermodified $cmnm^5Um34$ residue. In *Bacillus subtilis* and *Mycoplasma*

⌘ *Author's Choice*—Final version full access.

ˢ This article contains supplemental Tables S1 and S2 and an additional reference.

The atomic coordinates and structure factors (code 3VYW) have been deposited in the Protein Data Bank (http://wwpdb.org/).

[1] Holds the position of Emeritus Scientist at the CNRS, in the laboratory of Drs. Dominique Fourmy and Satoko Yoshizawa, France.

[2] To whom correspondence may be addressed: RIKEN Systems and Structural Biology Center, 1-7-22 Suehiro-cho, Tsurumi-ku, Yokohama, Kanagawa 230-0045, Japan. Tel.: 81-45-503-9196; Fax: 81-45-503-9195; E-mail: yokoyama@riken.jp.

[3] To whom correspondence may be addressed: RIKEN SPring-8 Center, Harima Institute, 1-1-1 Kouto, Sayo, Hyogo 679-5148, Japan. Tel.: 81-791-58-2891; Fax: 81-791-58-2892; E-mail: bessho@spring8.or.jp.

[4] The abbreviations used are: mnm^5s^2U, 5-methylaminomethyl-2-thiouridine; mnm^5U, 5-methylaminomethyluridine; $cmnm^5U$, 5-carboxymethylaminomethyl uridine; nm^5U, 5-aminomethyluridine; AdoMet, *S*-adenosylmethionine; MTase, methyltransferase; SeMet, selenomethionine.
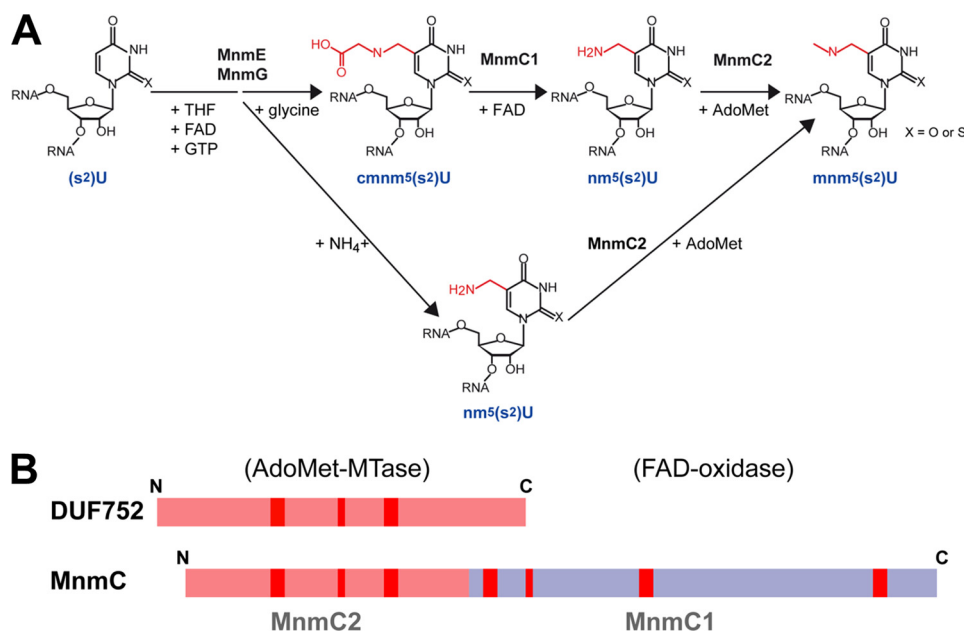
FIGURE 1. **mnm⁵U biosynthetic cascade in bacteria.** *A,* two proposed U34 modification pathways. *B,* schematic representations of the domain structures of *A. aeolicus* DFU752 and *E. coli* MnmC. The *coral pink* regions represent the AdoMet-dependent MTase domain, and the *blue* region represents the FAD-dependent oxidase domain. The *red* regions represent the conserved motifs in each domain.

capricolum, only cmnm⁵(s²)U(m)-type derivatives are found in the split codon box tRNAs (2, 4, 5), although in the majority of other bacteria the chemical identity of the wobble U34 is often not known. Finally, mammalian mitochondrial tRNAs contain a taurine derivative (τm⁵(s²)U34) (6, 7). These various derivatives of the wobble nucleoside are collectively designated as Xm⁵(s²)U(m), where X corresponds to distinct adducts of the minimal 5-methyluridine 34. Together with other modified nucleosides in the anticodon branch, they allow the modified tRNA to read selected mRNA codons more efficiently and accurately during translation on the ribosome (8–11).

Several enzymes catalyze the formation of Xm⁵U34 derivatives in *E. coli.* These include the GTPase MnmE (formerly designated as TrmE), the folate-dependent MnmG (GidA), and the bifunctional oxidase methyltransferase MnmC. The 2-thiolation is catalyzed by the thiolase MnmA, and the methyltransferase TrmL mediates the 2′-hydroxyl methylation of U34, regardless of whether the C5 atom of U34 is modified (12). Two alternative mechanisms have been proposed for the multistep enzymatic formation of mnm⁵U34 in tRNA (Fig. 1A). In the first pathway, the formation of 5-carboxymethylaminomethyluridine is catalyzed by MnmE and MnmG, using glycine, a methyl derivative of tetrahydrofolate, GTP, and FAD as cofactors. This complex reaction has been recapitulated under *in vitro* conditions, using purified recombinant MnmE-MnmG enzymes. However, its detailed mechanism is still a matter of debate (13–18). In the last two enzymatic steps, the 5-cmnm adduct is converted to the 5-mnm derivative (mnm⁵U34) by the bifunctional protein MnmC (18–22). The C-terminal domain of this protein (designated as MnmC1) first catalyzes the transformation of the 5-cmnm adduct of U34 into a 5-aminomethyluridine intermediate (nm⁵U34), which is subsequently methylated to mnm⁵U34 by the methyltransferase of the N-terminal

domain (DUF752, designated as MnmC2), using AdoMet as the methyl donor (Fig. 1A, *upper part*). The nm⁵U34-containing tRNA intermediate usually does not accumulate in normal *E. coli* cells, except in certain mutants such as rel⁻, met⁻, or those defective in the MnmC2 activity (19, 20, 23, 24). In the second alternative "shortcut" pathway, recently discovered by Armengod and co-workers (17), ammonium, instead of glycine, is used by the MnmE-MnmG complex to catalyze the direct formation of nm⁵U34-containing tRNA, thus bypassing the need for the MnmC1 activity (Fig. 1A, *lower part*). This nm⁵U34-containing tRNA intermediate is further methylated into the same final mnm⁵U34 product as above by the MnmC2 domain of the bifunctional MnmC. This nm⁵U-to-mnm⁵U methylation reaction has been demonstrated to occur *in vitro,* using a purified recombinant MnmC enzyme defective in the MnmC1 activity, thus showing that each of the two enzymatic activities of the fusion MnmC protein can be uncoupled and work independently in trans-complementation types of experiments (21, 22, 24).

These observations prompted us to examine the situation in *Aquifex aeolicus.* This bacterial species has genes encoding the MnmE, MnmG, and MnmA but only has one gene encoding a shorter version of MnmC (DUF752). This gene appears to be the homolog of MnmC2, and it seems to lack the FAD oxidase (DAO)-like MnmC1 domain (Fig. 1B). In this study, we first analyzed the *A. aeolicus* tRNAs and confirmed the presence of the mnm⁵U34-containing tRNA species. We next showed that purified *A. aeolicus* monofunctional DUF752 binds tRNA and displays the expected methyltransferase activity *in vitro.* Finally, we determined the crystal structure of *A. aeolicus* DUF752, which revealed the interesting tRNA-binding characteristics of this newly identified bacterial methyltransferase.

EXPERIMENTAL PROCEDURES

Strains and Isolation of Bulk tRNA from A. aeolicus and B. subtilis—Bulk tRNA from *B. subtilis* strain 168 (wild type) was obtained as described previously (25). Bulk tRNA from *A. aeolicus* VF5 was obtained by the same procedure.

Protein Expression and Purification—The gene encoding the DUF752 protein (aq_1980, gi:15606976), corresponding to the putative methyltransferase MnmC2, was amplified via PCR using *A. aeolicus* VF5 genomic DNA and was cloned into the pET-11b expression vector (Merck Novagen). The expression vector was introduced into the *E. coli* BL-21(DE3) strain (Merck Novagen), and the recombinant strain was cultured in 2.5 liters of LB medium. The harvested cells were resuspended in 20 mM Tris-Cl buffer (pH 8.0), containing 300 mM NaCl, 5 mM MgCl$_2$, and 2 mM DTT, and subsequently lysed by sonication four times for 30 s on ice (VP-30, TAITEC). After centrifugation at $27,000 \times g$ for 30 min (CR22GIII, Hitachi), the supernatants were heat-treated at 70 °C for 30 min and purified by a series of HiTrap-phenyl, HiTrap-Q, and Resource-S (GE Healthcare) column chromatography steps, followed by dialysis against 20 mM Tris-Cl buffer (pH 8.0), containing 150 mM NaCl and 2 mM DTT. The protein sample was then purified by gel filtration on a Superdex 75 10/300GL column (GE Healthcare) and was concentrated by centrifugal filtration (Millipore) to 11.3 mg/ml

For the x-ray crystallization experiment, the selenomethionine-labeled (SeMet) *A. aeolicus* DUF752 protein was obtained by expression from the same pET-11b expression vector, in the methionine-auxotrophic *E. coli* B834(DE3) strain cultured with SeMet, instead of methionine. The protein was purified in the same manner as that for the nonlabeled proteins.

For the Biacore binding assays, the Bio-tagged version of the *A. aeolicus* DUF752 protein was obtained by expression from the pET-11b vector (Merck Novagen) bearing the tag sequence at the N terminus (26), and the protein was purified in the same manner as the native proteins. The purified protein was then biotinylated by an incubation with *E. coli* biotin ligase, BirA, and biotin at 37 °C for 2 h.

The gene encoding MnmG (aq_761, gi:15606146) from *A. aeolicus* VF5 was cloned into pET-15b (Merck Novagen) and expressed in the *E. coli* Rosetta(DE3) strain (Merck Novagen). The harvested cells were resuspended in 50 mM HEPES buffer (pH 7.0), containing 500 mM NaCl, 500 mM MgCl$_2$, and 2 mM DTT. After sonication four times for 30 s (VP-30, TAITEC) and centrifugation at $15,000 \times g$ for 30 min (CR22GIII, Hitachi), the supernatant was heat-treated at 60 °C for 15 min and purified by a series of HisTrap, HiTrap-Q, and HiTrap-heparin (GE Healthcare) column chromatography steps. After the last chromatography step, the sample buffer was exchanged by dialysis at 4 °C to 50 mM HEPES buffer (pH 7.0), containing 150 mM NaCl and 2 mM DTT. The protein sample was then purified by gel filtration on a Superdex 75 10/300GL column (GE Healthcare) and was concentrated by centrifugal filtration (Millipore) to 3.3 mg/ml.

The gene encoding *A. aeolicus* MnmE (aq_871, gi:15606214) was cloned into pET-11b (Merck Novagen) and expressed in *E. coli* Rosetta(DE3) strain (Merck Novagen). The harvested

cells were resuspended in 20 mM Tris-Cl buffer (pH 8.0), containing 500 mM NaCl, 2 mM DTT, and 1 mM PMSF. After sonication four times for 30 s (VP-30, TAITEC) and centrifugation at $15,000 \times g$ for 30 min (CR22GIII, Hitachi), the supernatants were heat-treated at 75 °C for 15 min and purified by a series HiTrap-Q, HiTrap-heparin, and Resource-Q (GE Healthcare) column chromatography steps. The sample buffer was exchanged by dialysis at 4 °C to 20 mM Tris-Cl buffer (pH 8.0), containing 300 mM NaCl and 2 mM DTT. The protein sample was then purified by gel filtration on a Superdex 75 10/300GL column (GE Healthcare) and was concentrated by centrifugal filtration (Millipore) to 7.6 mg/ml.

The gene encoding MnmC (JW5380, gi: 85675355) from *E. coli* was cloned into pET-15b (Merck Novagen) and expressed in the *E. coli* Rosetta2(DE3) strain (Merck Novagen). The expression vector containing MnmC, bearing a mutation in the essential Asp-178 (D178A), was prepared using a QuikChange™ site-directed mutagenesis kit (Stratagene) and expressed in the same *E. coli* Rosetta2(DE3) strain (Merck Novagen). The purification procedures for these recombinant proteins were described previously (27).

Crystallization and Data Collection—For the crystallization assay, the purified *A. aeolicus* DUF752 protein samples were first concentrated to 13–26 mg/ml in 20 mM Tris-Cl buffer (pH 8.0), containing 150 mM NaCl and 2 mM DTT. The SeMet DUF752 protein was co-crystallized with 1 mM AdoMet by the hanging-drop vapor diffusion method. Preliminary screenings were performed using the Hampton Research Index Screen kit, and small crystals appeared with a reservoir solution consisting of 0.1 M sodium acetate buffer (pH 4.5), containing 25%(w/v) PEG 3350. After optimization, large crystals were obtained, using a reservoir solution of 0.1 M sodium acetate buffer (pH 5.0), containing 25%(w/v) PEG3350 and 5%(w/v) benzamidine. Rectangular parallel-piped crystals grew to dimensions of $0.2 \times 0.1 \times 0.1$ mm at 20 °C in 10 days. For data collection, the crystals were flash-cooled in liquid nitrogen with 13% glycerol as a cryoprotectant. Diffraction data sets were collected at the BL41XU beamline at SPring-8 (Harima, Japan) and were processed by the use of the HKL2000 software suite.

Structure Determination and Refinement—The structure of the *A. aeolicus* DUF752 protein was determined by using the SeMet MAD data set, SOLVE and RESOLVE (28). We used the second data set (peak 2), obtained from another crystal in the same crystallization drop, to improve the electron density map. The model (2.5 Å) was built and refined with NCS restraints by using the programs Coot (29) and Refmac5 implemented in the CCP4 suite (30). Data collection and refinement statistics are summarized in Table 1. The quality of the protein model was inspected by PROCHECK (31). Structure representations were prepared with the PyMOL program (Schrödinger, LLC.). Coordinates and structure factors have been deposited in the Protein Data Bank, with the accession code 3VYW.

MTase Activity of A. aeolicus DUF752—All assays were performed at 45 °C in a 300-μl reaction mixture containing 40 mM PIPES (pH 6.4), 20 mM NH$_4$Cl, 0.2 mM EDTA, 0.2 mM DTT, 20 μM FAD, 4 μM *S*-adenosyl-L-[*methyl*-^{14}C]methionine (2.22 GBq/mmol; GE Healthcare), 0.55 mg/ml (~20 μM) *B. subtilis* total tRNA (in which the C5 atom of several tRNAs harbors a

TABLE 1

Data collection, phasing, and refinement statistics

Values in parentheses are for highest resolution shell. r.m.s.d. means root mean square deviation.

	Peak	Edge	Remote	Peak 2
Data set				
X-ray source		SPring-8 BL41XU		SPring-8 BL41XU
Wavelength (Å)	0.9792	0.9795	0.9750	0.9792
Resolution (Å)	45–2.5	45–2.5	45–2.5	45–2.5
Cell parameters				
a (Å)	55.42	55.42	55.42	55.49
b (Å)	108.04	108.07	108.10	107.58
c (Å)	117.76	117.79	117.85	117.71
β	102.19°	102.18°	102.16°	102.44°
Space group	$P2_1$			$P2_1$
Molecules/asymmetric unit	4			4
Unique reflections	47,010	46,996	46,903	47,040
Redundancy	4.2	4.2	4.2	4.1
Completeness (%)	99.9 (100%)	99.9 (100)	99.9 (100)	99.8 (99.9)
$I/\sigma(I)$	16.9 (2.7)	17.4 (2.9)	17.2 (2.5)	19.5 (3.9)
Phasing				
Resolution (Å)	20.0–2.5			20.0–2.5
No. of sites	8			
Figure of merit	0.25 (after solvent modification, 0.57)			
Refinement				
Resolution range (Å)				45.4–2.5
R_{work}[a]/R_{free}[b] (%)				19.1/25.5
No. of protein atoms				10,068
No. of hetero atoms				126
No. of water molecules				146
r.m.s.d. bond lengths (Å)				0.028
r.m.s.d. bond angles				2.123°
Average B-value (Å^2)				50.89
Ramachandran plot (%)				
Core				94.1
Allowed				5.9

[a] $R_{\text{work}} = \Sigma|F_o - F_c|/\Sigma\,F_o|$.
[b] R_{free} is the same as R_{work} but calculated using a small fraction (5%) of randomly selected reflections.

wobble cmnm^5(s^2)U(m)34), 0.5 μM *E. coli* monofunctional MnmC-D178A mutant enzyme, and 5 μM *A. aeolicus* DUF752 protein. The *E. coli* mutant enzyme was used for producing the nm^{5}U-containing tRNA, which is the expected substrate of DUF752 (see under "Results"). At appropriate time points, 30-μl aliquots of the samples were mixed with a 20-fold volume of 10% cold trichloroacetic acid (TCA) and were incubated for 10 min on ice. The quenched samples were spotted on MF-Millipore membrane papers. The filters were washed five times with cold 10% TCA, and the radioactivity retained on the filter was measured with a liquid scintillation counter. The reactions were repeated five times, and the values were used to calculate the standard errors.

Enzyme-RNA Binding Assay—The interactions between the tRNA and the enzymes were analyzed with a Biacore 3000 SPR bio-sensor (GE Healthcare). The gene encoding the tRNA$^{\text{Lys}}_{\text{UUU}}$ from *A. aeolicus* (aq_t42, gene ID: 3284557) was amplified via PCR, using a 5′-primer including a T7 promoter and a 3′-primer lacking six nucleotides of the terminus. The biotinylated tRNA was prepared by enzymatically connecting the T7 transcripts, lacking six nucleotides of the 3′ terminus, and the synthesized 5′-p-TCACCA-biotin-3′ oligonucleotide DNA. The 3′-terminal biotinylated tRNA and the *A. aeolicus* DUF752 protein (MnmC2) were immobilized onto commercially prepared Biacore SA sensor chips, to yield analytes with R_{max} in the range of 500–1,400 resonance units. All subsequent binding experiments were performed in 20 mM HEPES buffer (pH 7.2), containing 200 mM NaCl and 10 mM MgCl$_2$. Each binding assay utilized 25–2,000 nM protein as the analyte, increased in at least

five steps, at a flow rate of 20 μl/min for 3 min. All binding assays were performed at 25 °C. The kinetic parameters and the dissociation constants (K_D) were determined from the sensorgram data, using the BIAevaluation 4.1 software package.

Analysis of tRNA Modification by High Performance Liquid Chromatography—The purified tRNAs were digested to nucleosides, as described previously (32), and were analyzed by HPLC (Alliance, Waters) using a Develosil 5-μm RP-AQUEOUS C-30 reverse phase column (Phenomenex). The elution was monitored at 254 and 314 nm, and the gradient was employed as described previously (32, 33). The thiolated nucleosides s^{2}C, mnm^{5}s^{2}U, and cmnm^{5}s^{2}U were identified by both their spectra and relative retention times to that of s^{4}U and were compared with the relative retention times of the corresponding synthetic nucleosides. The identification of m^{5}s^{2}U is described under "Results" and the legend to Fig. 5.

RESULTS

Comparison of Sequences and Domains—The amino acid sequence alignments of *A. aeolicus* DUF752 (*upper line*, 308 amino acids) and the N-terminal domains (254 amino acids) of the *E. coli* bifunctional MnmC methyltransferase (*bottom line*, 254 plus 414 amino acids) are shown in Fig. 2. A few additional homologous sequences from other organisms are also included between these two sequences (we also analyzed many others, data not shown). The high sequence similarity and the conservation of several key amino acids (nine altogether) suggested that both types of proteins possess similar and possibly identical functions. The sequence identity between *A. aeolicus*
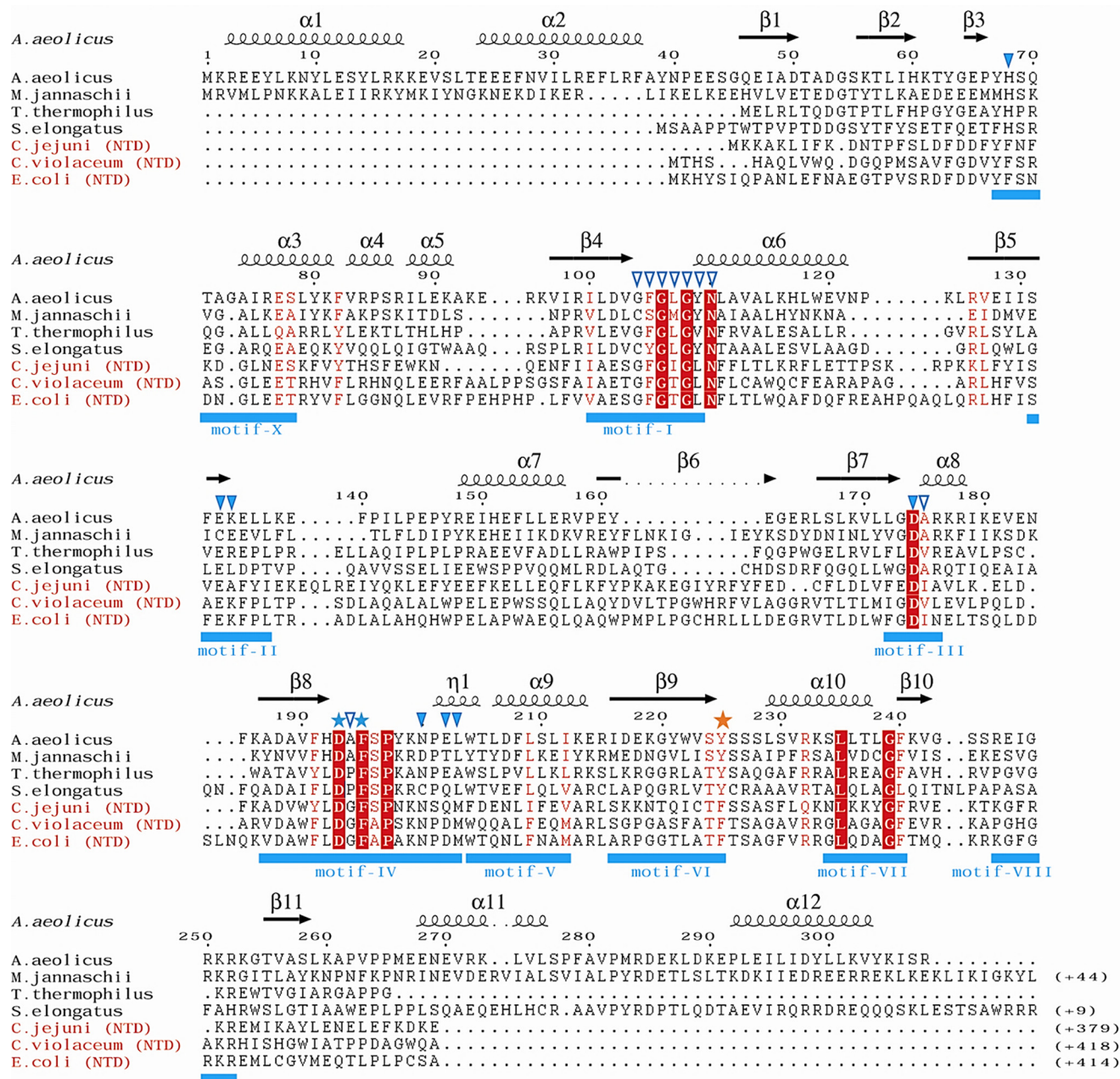
FIGURE 2. **Sequence alignment of DUF752, other homologous proteins, and the N-terminal domain of MnmC2 of the bifunctional MnmC.** The sequence alignment was created with ESPript (51). Conserved residues are colored *red*. The highly conserved residues are represented by *white letters* within *red rectangles*. The conserved motifs in the class I MTases are *underlined* by *heavy blue lines*. The signature motif D*X*F in motif IV is indicated by *blue stars*. The *orange star* indicates the residue proposed to interact with the substrate RNA. Residues interacting with the cofactor, AdoMet, are indicated by *blue triangles*. *Filled triangles* represent the residues interacting through side chains, and *empty triangles* represent the residues interacting through backbones. GI numbers are given in parentheses as follows: *A. aeolicus* VF5 (15606976); *Methanocaldococcus jannaschii* DSM 2661 (15668851); *T. thermophilus* HB8 (55980847); *Synechococcus elongatus* PCC 7942 (81300750); *Campylobacter jejuni* subsp. *jejuni* NCTC 11168 (218562880); *Chromobacterium violaceum* ATCC 12472 (34497397); *E. coli* str. K-12 substr. W3110 (85675355).

DUF752 and *E. coli* MnmC2 is 26%, despite the fact that these two proteins are from species that grow at very different optimal temperatures (above 40 °C and optimally at 85–95 °C in the case of the thermophilic *A. aeolicus* and below 40 °C and optimally at 37 °C in the case of *E. coli*). The MnmC2 domains (N-terminal domains) of the bifunctional MnmC and DUF752 homologs both show the typical features of the AdoMet-dependent class I (Rossmann-fold) MTase family (motifs X and I–VIII, *underlined* in *blue* in Fig. 2) (34). The features include

the partially conserved (G*X*)G*X*G sequence within motif I, followed by a conserved Asn residue at the end of the β4 region. In many class I MTases, including the N-terminal domain of MnmC and the present *A. aeolicus* DUF752, this motif constitutes an essential element of the nucleotide binding pocket (27).

Overall Structure of DUF752—The overall tertiary structure of monomeric *A. aeolicus* DUF752, determined at 2.5 Å resolution, shows a central core domain with the canonical secondary structure characteristic of the class I MTases, with additional
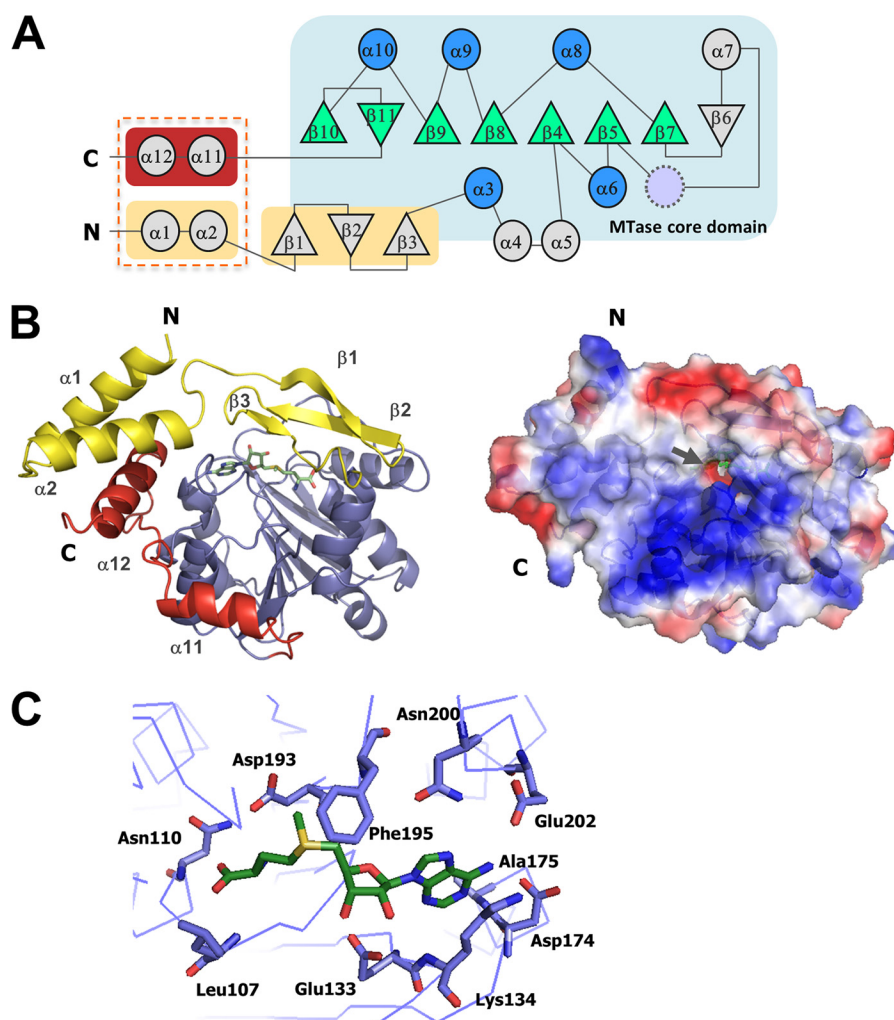
FIGURE 3. **Crystal structure of *A. aeolicus* DUF752.** *A,* schematic representation of the topology of *A. aeolicus* DUF752. The *blue-colored* region represents the central core domain of the class I MTase. The additional N- and C-terminal regions are colored *yellow* and *red*, respectively. The *red dashed box* shows the extra terminal modules specific to DUF752 (*cf.* Fig. 6*A*). *B,* crystal structures of *A. aeolicus* DUF752 bound to AdoMet. The color scheme in the *left panel* is the same as that in *A*. The *right panel* shows the electrostatic surface representation, generated by PyMOL quasi-Coulombic calculation (contoured at ± 74.647 *kT/e*), in which *blue* indicates positive charges, and *red* indicates negative charges. The *arrow* shows the location of the AdoMet cofactor within the methyltransferase domain. *C,* details of the AdoMet-binding site.

N- and C-terminal modules (Fig. 3, compare *A* and *B*). The additional N-terminal module (in *yellow* in Fig. 3) consists of two α-helices and three β-strands, whereas the C-terminal module (in *red* in Fig. 3) consists of two α-helices. The α-helices of both termini are close together (Fig. 3, *A* and *B*). The β-sheet (β1 to β3) with α1 and α2 in the N-terminal module surround the cofactor, AdoMet, along with the MTase fold (see below). In fact, this β-sheet covers the AdoMet binding pocket and limits cofactor access to the solvent (see *arrow* in Fig. 3*B*). This feature is characteristic of DUF752 and all of the MnmC2 family proteins we examined (Fig. 2). In contrast, in other tRNA methyltransferases, the AdoMet is usually exposed to the solvent. The C-terminal extra sequence (α11 and α12) of DUF752 may form part of the tRNA binding pocket, in which charged residues and aromatic amino acids could play important roles in tRNA recognition and/or binding.

A DALI search confirmed that the MTase domain (*blue background* in Fig. 3*A*) shares high similarity with the N-terminal (MnmC2) domain of the bifunctional *E. coli* MnmC we reported previously (supplemental Table S1) (27). However, a few other MTases also show significant structural similarities, including guanidinoacetate *N*-methyltransferase interacting with a small cellular metabolite and various MTases interacting with RNA, such as TrmI (tRNA-m^{1}A58 *N*-methyltransferase), mRNA cap guanine-N7 methyltransferase, RsmC (16 S rRNA-m^{2}G1207 *N*-methyltransferase), and Trm1 (tRNA-m$^2_2$G *N*-methyltransferase (supplemental Table S1).

Within this methyltransferase domain, the residues constituting the AdoMet binding pocket are well conserved between DUF752 and the MnmC2 domain of the bifunctional MnmC. As shown in Fig. 3*C*, a network of amino acid interactions facilitates the recognition of the cofactor. The amino acids that are close by and/or interacting with a given atom of AdoMet are listed in supplemental Table S2, and most of them are indicated by *triangles* in Fig. 2. Notably, the carboxyl group in the methionine moiety is recognized by the enzyme backbone from residues Leu-107 to Asn-110, which compose part of the conserved (G*X*)G*X*G*X*N in motif I (Fig. 2). The N1 position of the adenine moiety is recognized by a hydrogen bond with the backbone of Ala-175 in motif III, whereas the amino group (N6)

in the adenine is recognized by the side chains of the conserved Asp-174 in motif III and Glu-202 in motif IV. Furthermore, the N7 position of the adenine ring hydrogen bonds with the side chain of Asn-200, adjacent to the conserved DXFXP sequence in motif IV. The 2′- and 3′-hydroxyl groups of the ribose moiety of AdoMet are recognized by the partially conserved Glu-133 in motif II. The location of the carboxyl group of the conserved Asp-193 probably allows the formation of a hydrogen bond with the amino group in the AdoMet. Finally, the base moiety of AdoMet stacks on Lys-134, located in signature motif II (Fig. 3*C*).

In summary, the overall structure of *A. aeolicus* DUF752, in complex with its cofactor AdoMet, is very similar to that of the MnmC2 domain of *E. coli* MnmC, as we determined previously (27). All of the observations mentioned above support the idea that the monofunctional methyltransferase DUF752 of *A. aeolicus* functions in a similar manner to *E. coli* MnmC2, fused to its oxidase domain MnmC1, in the bifunctional MnmC.

MTase Activity of DUF752—To further investigate whether *A. aeolicus* DUF752 functions in the same manner as the *E. coli* MnmC2 enzyme, the MTase activity was monitored *in vitro*, using the purified recombinant enzyme, radiolabeled AdoMet as the methyl donor and bulk *B. subtilis* tRNA as the substrate. Because *B. subtilis* lacks a gene encoding either MnmC or a "stand-alone" MnmC1 (FAD oxidase domain), but possesses genes encoding the MnmE, MnmG, MnmA, and TrmL proteins (35), cmnm⁵(s²)U and cmnm⁵Um derivatives are present at the wobble position 34 of its tRNAs (2, 4). Considering the fact that the enzymatic activities of the bifunctional *E. coli* MnmC can be decoupled *in vitro* (22, 24), the cmnm⁵(s²)U(m) derivatives were converted to suitable nm⁵(s²)U(m)-34-containing tRNA substrates, by simply incubating the bulk *B. subtilis* tRNA with the purified recombinant mutant *E. coli* MnmC (D178A). This Asp-to-Ala mutation in *E. coli* MnmC (corresponding to Asp-193 in *A. aeolicus* DUF752) was shown to severely reduce the methyltransferase activity of MnmC2, although the full activity of the FAD oxidase MnmC1 is retained (22, 24).

All of the MTase activities were tested at 45 °C. Two control experiments were performed as follows: one in the presence of only the *E. coli* mutant MnmC (D178A) together with its cofactor FAD and the second in the presence of only the *A. aeolicus* DUF752. Under these experimental conditions, the MTase activities of both the *E. coli* mutant MnmC (D178A) and the *A. aeolicus* DUF752 protein were almost nonexistent. Substantial MTase activity was only evident in the presence of both the *E. coli* mutant MnmC (D178A) and the *A. aeolicus* DUF752 (Fig. 4). The methyltransferase activity of DUF752 corresponds to the methylation of the fraction of nm⁵(s²)U34, generated from cmnm⁵(s²)U-containing *B. subtilis* tRNA by the FAD oxidase activity of the MnmC1 domain of the *E. coli* mutant MnmC (D178A) (Fig. 1*A*).

To confirm the direct interaction of DUF752 with the tRNA substrate, we next performed an *in vitro* binding assay, using Biacore surface plasmon resonance (Table 2). In this experiment, a biotinylated T7 transcript of the *A. aeolicus* tRNA^Lys gene was used as the substrate and immobilized on a series of sensor chips. Various concentrations of the analyte DUF752 were then flowed through the capillary tubes, although the temperature was maintained at 25 °C. A dissociation constant of
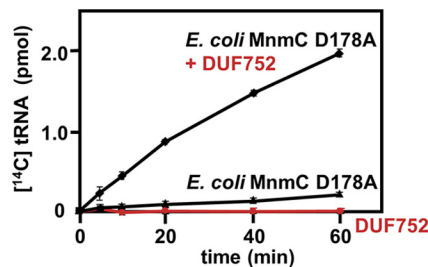

FIGURE 4. **Measurements of MTase activities *in vitro*.** A quantitative diagram of the time courses of the MTase assays. The reactions were performed with unlabeled *B. subtilis* total tRNA and [¹⁴C]AdoMet. Experimental details are provided under "Experimental Procedures" and the text.

1,970 nM was obtained, which is reasonable considering that the tRNA transcript is probably not an optimal substrate, *i.e.* it lacks all modified bases, including the aminomethyl (nm) group on the C5 atom of the uracil ring at the wobble position of tRNA. The same biotinylated T7- transcript of *A. aeolicus* tRNA^Lys was also tested with purified recombinant *A. aeolicus* MnmE and MnmG as analytes, and dissociation constants of 47.0 nM for MnmE and 62.7 nM for MnmG were obtained (Table 2). When DUF752 instead of biotinylated tRNA^Lys was linked on the sensor chip and the same recombinant MnmE and MnmG were used as analytes, dissociation constants of 61.4 and 82.2 nM were obtained, respectively.

In summary, these results demonstrated that *A. aeolicus* DUF752 functions as a tRNA methyltransferase in spite of the absence of a fused FAD oxidase domain, as long as a suitable nm⁵U-containing tRNA substrate is present in the reaction mixture. They also suggested that, during the sequential enzymatic formation of the 5-mnm adduct on the C5 atom of U34 in tRNA, DUF752 could, at least transiently, associate with the MnmE-MnmG complex.

DUF752 Methylates tRNA in Vivo—To determine whether DUF752 also functions as an active tRNA methyltransferase *in vivo*, we next identified the chemical group attached to the C5 atom of a subset of s²U34-containing tRNA of *A. aeolicus*, and we compared it with those on the nucleosides of the same subset of *E. coli* tRNA. Total tRNA was purified from full-grown cultures of *E. coli*, *A. aeolicus*, and as a control a Δ*mnmC*::*Amp E. coli* strain lacking the *mnmC* gene. Bulk tRNAs from these three bacteria were then analyzed by HPLC, after digestion of the tRNA to nucleosides. The concentration of the nucleosides was monitored at 314 nm to detect the thiolated nucleosides preferentially. The chromatographic profile (Fig. 5*A*) revealed that the hydrolysate of total tRNA purified from the *E. coli* wild type mainly contains three different thiolated nucleosides. The s²C and s⁴U nucleosides are expected from their presence in certain tRNAs at positions 32 and 8, respectively (2). The only s²U derivative was mnm⁵s²U, which is derived from the combined actions of MnmE, MnmG, MnmA, and MnmC1+C2 of MnmC, during the maturation of tRNA^Gln, tRNA^Lys, and tRNA^Glu. One might expect the presence of a small amount of cmnm⁵ derivatives. However, as demonstrated previously by Hagervall *et al.* (20), the formation of this intermediate is sensitive to the growth conditions and the strain. For example, when a low sulfate concentration is present in the growth medium, the wild-type *E. coli* contains 21% cmnm⁵s²U and 79%

TABLE 2

Binding affinities of *A. aeolicus* tRNA^{Lys}, DUF752 (MnmC2), MnmE, and MnmG, determined by Biacore analyses

Ligand	Analyte	k_a	k_d	K_D	Fitting model
		$M^{-1}s^{-1}$	s^{-1}	M	
tRNA^{Lys}	MnmC2	$(8.65 \pm 0.30) \times 10^3$	$(1.71 \pm 0.02) \times 10^{-2}$	1.97×10^{-6}	1:1 binding
tRNA^{Lys}	MnmE	$(7.21 \pm 0.12) \times 10^4$	$(3.39 \pm 0.20) \times 10^{-3}$	4.70×10^{-8}	1:1 binding
tRNA^{Lys}	MnmG	$(7.83 \pm 0.16) \times 10^4$	$(4.91 \pm 0.07) \times 10^{-3}$	6.27×10^{-8}	1:1 binding
MnmC2	MnmE	$(8.95 \pm 0.11) \times 10^4$	$(5.50 \pm 0.11) \times 10^{-3}$	6.14×10^{-8}	1:1 binding
MnmC2	MnmG	$(1.13 \pm 0.02) \times 10^5$	$(9.26 \pm 0.20) \times 10^{-3}$	8.22×10^{-8}	1:1 binding

mnm^{5}s^{2}U but no nm^{5}s^{2}U. In wild-type *Salmonella enterica* grown logarithmically in rich medium, only a small amount of cmnm^{5}s^{2}U was observed, originating from tRNA^{Gln} (36). Thus, wild-type *E. coli* has the capacity to synthesize cmnm^{5}s^{2}U, and its subsequent enzymatic transformation is sensitive to the physiological conditions and the substrate tRNA. Because the nm^{5}s^{2}U intermediate is rarely observed, one can conclude that under *in vivo* conditions it is quickly converted to the mature mnm^{5}s^{2}U, a situation that is consistent with the *in vitro* methylation reaction occurring more quickly than the cleavage reaction (22, 24). In contrast, in the hydrolysate derived from tRNA isolated from the Δ*mnmC::Amp E. coli* strain, only the intermediate product cmnm^{5}s^{2}U was evident, whereas no mnm^{5}s^{2}U was detected (Fig. 5*B*). Thus, by abolishing the activity of the MnmC enzyme, the cmnm^{5}s^{2}U intermediate accumulates in *E. coli*, a situation one would expect in any organism lacking the bifunctional *mnmC* gene, if the glycine pathway was operating (Fig. 1*A*, *upper pathway*).

An interesting result is shown in Fig. 5*C*, where despite the absence of the bifunctional *mnmC* gene in the *A. aeolicus* genome the only s^{2}U derivative present, besides the expected m^{5}s^{2}U, was mnm^{5}s^{2}U, and notably, no cmnm^{5}s^{2}U was detected. This result allowed us to conclude that, in contrast to the situation in *E. coli* (12), in *A. aeolicus* the intermediate nm^{5}s^{2}U34 is the major product catalyzed by the enzymes MnmE, MnmG, and MnmA, and in turn it becomes fully methylated to the final derivative mnm^{5}s^{2}U via the ammonium pathway depicted in Fig. 1*A* (*lower part*). Because no traces of cmnm^{5}s^{2}U could be detected in the tRNA originating from *A. aeolicus* (Fig. 5*C*), the production of this intermediate by the alternative glycine pathway is obviously insignificant (Fig. 1*A*, *upper part*).

The large peak eluting after s^{4}U in Fig. 5*C* corresponds to m^{5}s^{2}U (s^{2}T), which was demonstrated to exist at position 54 in the T loop of tRNA isoacceptors in thermophilic organisms, such as *Thermus thermophilus* (37) and *Pyrococcus furiosus* (38), and obviously also in *A. aeolicus* (this work). As a matter of fact, the *A. aeolicus* genome contains the *trmFO* and *ttuA* genes, which encode a tRNA-m^{5}U54 methyltransferase (25) and a tRNA U54 thiolase (39), respectively.

DISCUSSION

In A. aeolicus, the Major Route for Enzymatic Formation of mnm^{5}U34 Depends on Use of Ammonium Rather Than Glycine—We showed that the *A. aeolicus* DUF752 protein is a homolog of the MnmC2 domain of the bifunctional *E. coli* MnmC and shares the same cellular function. Not only are the sequences and structures very similar but also the purified recombinant DUF752 catalyzes the same methylation reaction

in vitro as the MnmC2 domain of the *E. coli* bifunctional MnmC. Despite the absence of the FAD-dependent oxidase MnmC1 homolog, the *A. aeolicus* tRNA contains the same mnm^{5}s^{2}U34 modification as in tRNAs from other bacteria encoding the bifunctional *mnmC* gene. These observations strongly support the recent results showing that in *E. coli* two alternative pathways exist for the biosynthesis of the mnm^{5}U34 derivative. One mainly uses glycine as a cofactor and requires the combined activities of the FAD-dependent MnmC1 plus the methyltransferase MnmC2, and a second minor one, identified only under special experimental conditions, uses ammonium as a cofactor and requires the MnmC2 methyltransferase activity (Fig. 1*A*) (12, 17).

Given the complete absence of cmnm^{5}s^{2}U34 in bulk *A. aeolicus* tRNA (Fig. 5*C*), we concluded that in *A. aeolicus*, and probably in other bacteria lacking the gene encoding an MnmC1 homolog, the shortcut ammonium-dependent metabolic pathway is prevalent. In addition, because the tRNA harboring the nm^{5}s^{2}U modification does not accumulate in either wild-type *E. coli* or *A. aeolicus* (Fig. 5), under the usual laboratory experimental conditions for cell growth, the nm^5(s^2)U34 derivative either does not accumulate or is rapidly methylated by the MnmC2/DUF752 enzyme. The same situation existed when recombinant *E. coli* MnmC or a mixture of the MnmC1 and MnmC2 domains of *E. coli* were tested under *in vitro* conditions (22, 24). In addition, consistent with the finding that the nm^{5}s^{2}U intermediate is rarely observed in tRNA (22), the *in vitro* methylation reaction was shown to be much faster than the cleavage reaction (24).

The *M. capricolum* and *B. subtilis* genomes lack the genes encoding the bifunctional MnmC protein or a monofunctional MnmC2. Instead, they encode the MnmE, MnmG, MnmA, and TrmL enzymes (35, 40). In these bacteria, the C5 atom of the wobble U34 of the tRNAs specific for Gln, Lys, Glu, Arg, Gly, and Leu were shown to harbor only cmnm^{5}U, cmnm^{5}s^{2}U, or cmnm^{5}Um derivatives (4, 5). The glycine-dependent metabolic pathway (Fig. 1*A*, *upper part*) is obviously the dominant route used by these bacteria. The situation in mammalian mitochondria is similar, except that taurine, instead of glycine, is used by the GTPBP3/MTO1 enzymes, the homologs of bacterial MnmE-MnmG, to catalyze τm^{5}U34 and τm^{5}s^{2}U34 formation in a subset of their tRNAs (6, 41). Evidently, the type of biosynthetic pathway leading to Xm^{5}U34 derivatives in a subset of tRNAs strongly depends on the organism and the organelles considered and probably the physiological/environmental growth conditions of the cells as well.

Conserved Aspartic Acid Residue in the DUF752/MnmC2 Enzyme Plays an Essential Role in the Methylation Reaction, as
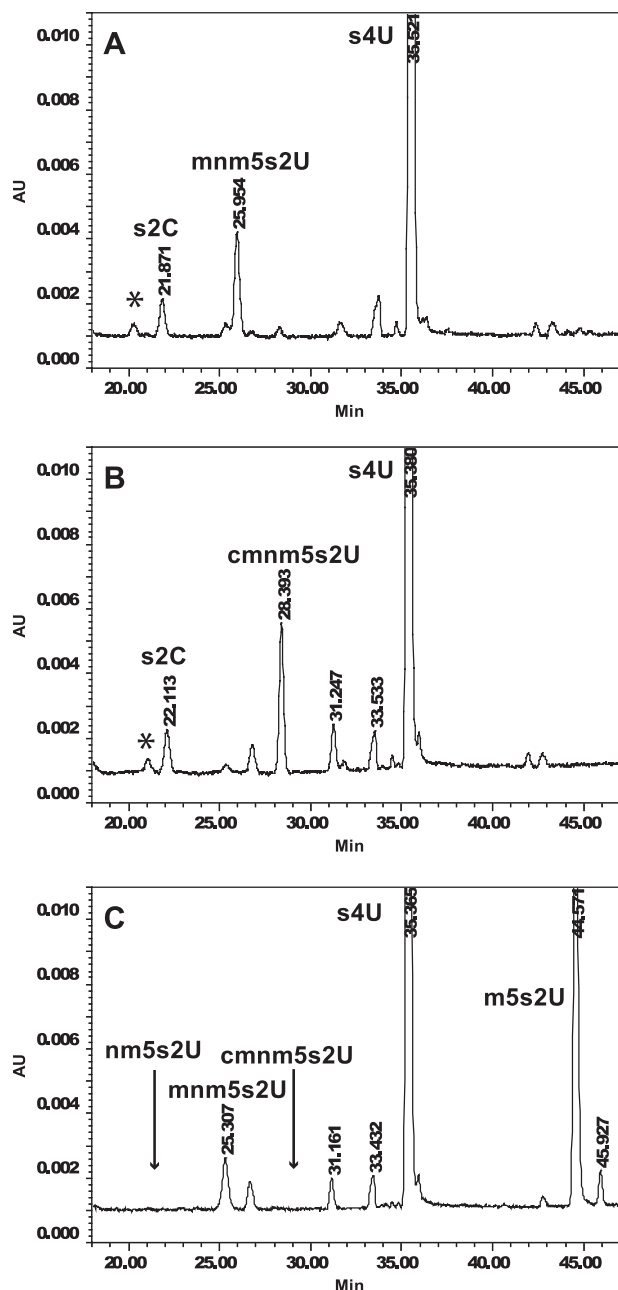
FIGURE 5. **HPLC analyses of naturally occurring cellular bulk tRNA.** HPLCs monitored at 314 nm of nucleosides originated from bulk tRNA preparations from wild-type *E. coli* (*A*), Δ*mnmC::Amp E. coli* (*B*), and *A. aeolicus* (*C*). The identities of the three s^2U derivatives, mnm^5s^2U, $cmnm^5s^2U$, and nm^5s^2U, were established by their identical relative retention times to that of s^4U, as the synthetic marker. Moreover, they had identical spectra to those of the synthetic markers. A figure showing a similar analysis in the case of synthetic markers was presented previously (17). The identity of m^5s^2U (s^2T) is discussed under "Results," and its spectrum and relative retention time are identical to those published for m^5s^2U (17). The *asterisk* in *A* and *B* indicates compounds migrating in a similar manner to nm^5s^2U but with distinct spectra. The *arrows* in *C* indicate the positions where nm^5s^2U and $cmnm^5s^2U$ should migrate, as judged by the retention times of the synthetic markers of these nucleosides relative to that of s^4U.

in the Other Class I N-Methyltransferases—As mentioned above, the structure of *A. aeolicus* DUF752 is highly homologous to the N-terminal MnmC2 domain of the bifunctional *E. coli* MnmC-fused protein (Fig. 6A). The electrostatic potentials of DUF752 (Fig. 3B, *right panel*) and *E. coli* MnmC (27) indicated that
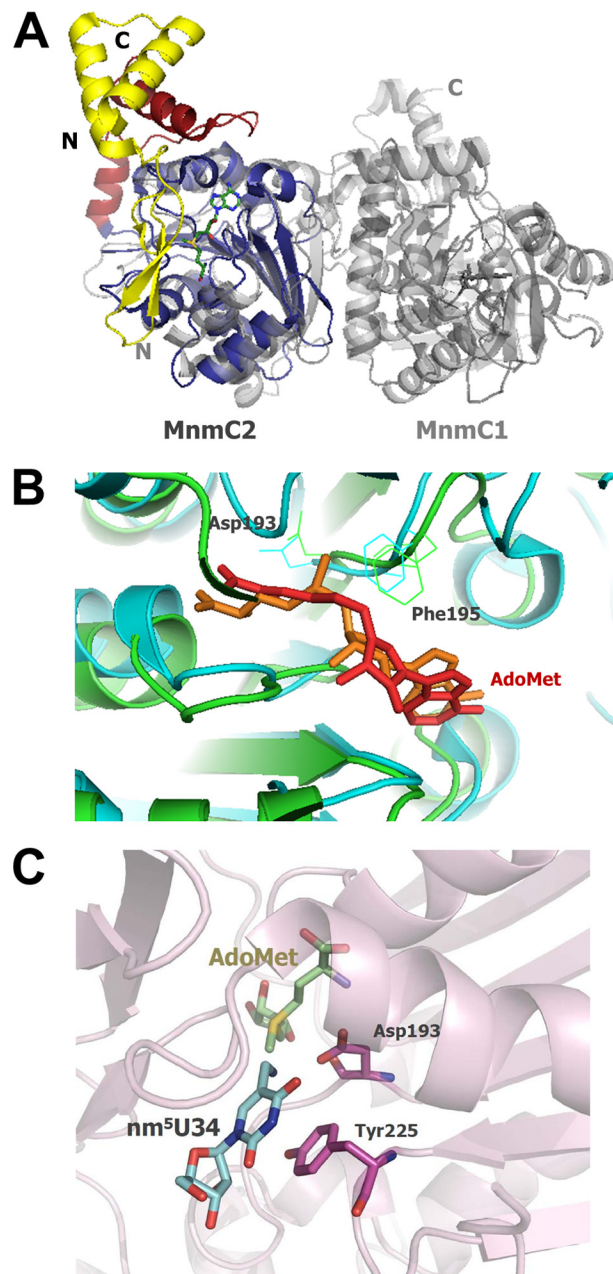

FIGURE 6. *A,* superimposition of *A. aeolicus* DUF752 on the *E. coli* MnmC-fused protein (Protein Data Bank code 3AWI). The color scheme of *A. aeolicus* DUF752 is the same as that in Fig. 3. The *E. coli* MnmC is colored *gray. B,* superimposition of *A. aeolicus* DUF752 on *P. horikoshii* Trm1 (Protein Data Bank code 2EJU), colored *green* and *blue,* respectively. The AdoMet cofactor bound to DUF752 is colored *red,* and the cofactor bound to Trm1 is colored *orange. C,* docking model of the DUF752 protein and the nm^5U substrate. The coordinates of nm^5U were generated by modifying 5-methylaminomethyl-2-thiouridine-5p-monophosphate (U8U) in the HIC-Up database (52).

tRNA binds to both proteins on the same side. Furthermore, they both possess the conserved D*X*F sequence in motif IV (Asp-193 and Phe-195 in *A. aeolicus* and Asp-178 and Phe-180 in *E. coli,* marked with *blue stars* in Fig. 2). This aspartic acid residue in the D*X*F sequence is highly conserved in all of the DUF752/MnmC2 sequences examined so far (Fig. 2) (21, 27).[5] In the crystal structures of DUF752 and the MnmC2 domain, this motif surrounds

---

[5] C. Brochier-Armanet, Y. Bessho, and H. Grosjean, unpublished results.

the methyl group donor of AdoMet (Fig. 3C). The corresponding region of many class I MTases involved in *N*-methylation reactions has a semi-conserved (D/N/S)PPY motif (34). In these MTases, the first (D/N/S) and the second proline residues form hydrogen bonds with the cofactor, with the nitrogen nucleophiles oriented toward the methyl group of AdoMet (34, 42, 43). Interestingly, the Trm1 protein, which also belongs to the class I *N*-methyltransferase family and catalyzes the dimethylation of the exocyclic amino group of the G26 residue in tRNAs (44–48), possesses a DPF motif (49). Based on the structure of *Pyrococcus horikoshii* Trm1, the first aspartic acid residue in the DPF motif was proposed to function as a nucleophile, by attracting one proton of the amino group of the target G26 (49). The superimposition of DUF752 on Trm1 indicated that the conformations of the AdoMet binding pockets of both proteins are similar (Fig. 6B), suggesting that the Asp-193 residue in the DAF motif of *A. aeolicus* DUF752 plays the same role as the corresponding residue in the DPF motif (Asp-138) of *P. horikoshii* Trm1. In this scenario, the carboxyl group of Asp-193 in DUF752 is a catalytic base that attracts the proton of the amino group of the nm^5U34-containing tRNA. In synergy with other active site amino acids, this Asp-193 residue could then catalyze the nucleophilic attack on the methyl moiety of AdoMet (Fig. 6C). Notably, the structure and the surface potential of *A. aeolicus* DUF752 are arranged in such a way that the nm^5U34-target base of tRNA enters the catalytic pocket from the opposite side of the proposed tRNA-binding sites in the *P. horikoshii* and *A. aeolicus* Trm1 enzymes (49, 50). In the Trm1 enzymes, the exocyclic amine group of the G26 target nucleoside of the tRNA is stabilized through a stacking interaction with a phenylalanine residue (Phe-140 in *P. horikoshii* and Phe-134 in *A. aeolicus*) in motif *X*. However, in the MnmC2/DUF752 family, it is more likely that the substrate is stabilized by a conserved Tyr (Tyr-225 in *A. aeolicus*) in motif VI (Fig. 6C), whereas a phenylalanine is prevalent at the corresponding position in MnmC2 of the bifunctional *E. coli* MnmC (Phe-210 in *E. coli*) (27). In the MnmC2/DUF752 family, the additional N- and C-terminal modules prevent the substrate tRNA from entering the catalytic pocket from the same side, as in the Trm1 enzymes. Instead, the MnmC2/DUF752 enzyme forms a possible tRNA-binding site on the other side, composed of the conserved positive residues (Fig. 3B, *right panel*). This narrow binding pocket leading to the AdoMet cofactor is considered to accommodate the longer 5-aminomethyl adduct of the substrate.

Taken together, the monofunctional DUF752 was proved to possess the same functional and structural properties as the MnmC2 domains of the bifunctional MnmC family of enzymes. Thus, we propose the designation of all of these bacterial enzymes with the same acronym, MnmC2.

REFERENCES

1. Grosjean, H. (2009) in *DNA and RNA Modification Enzymes* (Grosjean, H., ed) pp. 1–18, Landes Bioscience, Austin, TX
2. Jühling, F., Mörl, M., Hartmann, R. K., Sprinzl, M., Stadler, P. F., and Pütz, J. (2009) tRNAdb 2009. Compilation of tRNA sequences and tRNA genes. *Nucleic Acids Res.* **37**, D159–D162
3. Czerwoniec, A., Dunin-Horkawicz, S., Purta, E., Kaminska, K. H., Kasprzak, J. M., Bujnicki, J. M., Grosjean, H., and Rother, K. (2009) MODOMICS. A database of RNA modification pathways. 2008 update. *Nucleic Acids Res.* **37**, D118–D121
4. Yamada, Y., Murao, K., and Ishikura, H. (1981) 5-(Carboxymethylaminomethyl)-2-thiouridine, a new modified nucleoside found at the first letter position of the anticodon. *Nucleic Acids Res.* **9**, 1933–1939
5. Andachi, Y., Yamao, F., Muto, A., and Osawa, S. (1989) Codon recognition patterns as deduced from sequences of the complete set of transfer RNA species in *Mycoplasma capricolum*. Resemblance to mitochondria. *J. Mol. Biol.* **209**, 37–54
6. Suzuki, T., Suzuki, T., Wada, T., Saigo, K., and Watanabe, K. (2002) Taurine as a constituent of mitochondrial tRNAs. New insights into the functions of taurine and human mitochondrial diseases. *EMBO J.* **21**, 6581–6589
7. Umeda, N., Suzuki, T., Yukawa, M., Ohya, Y., Shindo, H., Watanabe, K., and Suzuki, T. (2005) Mitochondria-specific RNA-modifying enzymes responsible for the biosynthesis of the wobble base in mitochondrial tRNAs. Implications for the molecular pathogenesis of human mitochondrial diseases. *J. Biol. Chem.* **280**, 1613–1624
8. Björk, G. R., and Hagervall, T. G. (2005) in *EcoSal-Escherichia coli and Salmonella: Cellular and Molecular Biology* (Curtiss, R., 3rd., Böck, A., Ingraham, J. L., Kaper, J. B., Maloy, S., Neidhardt, F. C., Riley, M. M., Squires, C. L., and Wanner, B. L., eds) pp. 4.6.2, American Society for Microbiology, Washington, D. C.
9. Agris, P. F. (2008) Bringing order to translation. The contributions of transfer RNA anticodon-domain modifications. *EMBO Rep.* **9**, 629–635
10. Grosjean, H., de Crécy-Lagard, V., and Marck, C. (2010) Deciphering synonymous codons in the three domains of life. Co-evolution with specific tRNA modification enzymes. *FEBS Lett.* **584**, 252–264
11. Watanabe, K. (2010) Unique features of animal mitochondrial translation systems. The non-universal genetic code, unusual features of the translational apparatus, and their relevance to human mitochondrial diseases. *Proc. Jpn. Acad. Ser. B Phys. Biol. Sci.* **86**, 11–39
12. Armengod, M. E., Moukadiri, I., Prado, S., Ruiz-Partida, R., Benítez-Páez, A., Villarroya, M., Lomas, R., Garzón, M. J., Martínez-Zamora, A., Meseguer, S., and Navarro-González, C. (2012) Enzymology of tRNA modification in the bacterial MnmEG pathway. *Biochimie* **94**, 1510–1520
13. Yim, L., Moukadiri, I., Björk, G. R., and Armengod, M. E. (2006) Further insights into the tRNA modification process controlled by proteins MnmE and GidA of *Escherichia coli*. *Nucleic Acids Res.* **34**, 5892–5905
14. Meyer, S., Wittinghofer, A., and Versées, W. (2009) G-domain dimerization orchestrates the tRNA wobble modification reaction in the MnmE/GidA complex. *J. Mol. Biol.* **392**, 910–922
15. Shi, R., Villarroya, M., Ruiz-Partida, R., Li, Y., Proteau, A., Prado, S., Moukadiri, I., Benítez-Páez, A., Lomas, R., Wagner, J., Matte, A., Velázquez-Campoy, A., Armengod, M. E., and Cygler, M. (2009) Structure-function analysis of *Escherichia coli* MnmG (GidA), a highly conserved tRNA-modifying enzyme. *J. Bacteriol.* **191**, 7614–7619
16. Osawa, T., Ito, K., Inanaga, H., Nureki, O., Tomita, K., and Numata, T. (2009) Conserved cysteine residues of GidA are essential for biogenesis of 5-carboxymethylaminomethyluridine at tRNA anticodon. *Structure* **17**, 713–724
17. Moukadiri, I., Prado, S., Piera, J., Velázquez-Campoy, A., Björk, G. R., and Armengod, M. E. (2009) Evolutionarily conserved proteins MnmE and GidA catalyze the formation of two methyluridine derivatives at tRNA wobble positions. *Nucleic Acids Res.* **37**, 7177–7193
18. Bessho, Y., and Yokoyama, S. (2009) in *DNA and RNA Modification Enzymes* (Grosjean, H., ed) pp. 409–425, Landes Bioscience, Austin, TX
19. Taya, Y., and Nishimura, S. (1973) Biosynthesis of 5-methylaminomethyl-2-thiouridylate. I. Isolation of a new tRNA-methylase specific for 5-methylaminomethyl-2-thiouridylate. *Biochem. Biophys. Res. Commun.* **51**, 1062–1068
20. Hagervall, T. G., Edmonds, C. G., McCloskey, J. A., and Björk, G. R. (1987) Transfer RNA(5-methylaminomethyl-2-thiouridine)-methyltransferase from *Escherichia coli* K-12 has two enzymatic activities. *J. Biol. Chem.* **262**,

8488–8495

21. Bujnicki, J. M., Oudjama, Y., Roovers, M., Owczarek, S., Caillet, J., and Droogmans, L. (2004) Identification of a bifunctional enzyme MnmC involved in the biosynthesis of a hypermodified uridine in the wobble position of tRNA. *RNA* **10,** 1236–1242

22. Roovers, M., Oudjama, Y., Kaminska, K. H., Purta, E., Caillet, J., Droogmans, L., and Bujnicki, J. M. (2008) Sequence-structure-function analysis of the bifunctional enzyme MnmC that catalyses the last two steps in the biosynthesis of hypermodified nucleoside mnm^{5}s^{2}U in tRNA. *Proteins* **71,** 2076–2085

23. Elseviers, D., Petrullo, L. A., and Gallagher, P. J. (1984) Novel *E. coli* mutants deficient in biosynthesis of 5-methylaminomethyl-2-thiouridine. *Nucleic Acids Res.* **12,** 3521–3534

24. Pearson, D., and Carell, T. (2011) Assay of both activities of the bifunctional tRNA-modifying enzyme MnmC reveals a kinetic basis for selective full modification of cmnm^{5}s^{2}U to mnm^{5}s^{2}U. *Nucleic Acids Res.* **39,** 4818–4826

25. Urbonavicius, J., Brochier-Armanet, C., Skouloubris, S., Myllykallio, H., and Grosjean, H. (2007) *In vitro* detection of the enzymatic activity of folate-dependent tRNA (Uracil-54,-C5)-methyltransferase. Evolutionary implications. *Methods Enzymol.* **425,** 103–119

26. Tucker, J., and Grisshammer, R. (1996) Purification of a rat neurotensin receptor expressed in *Escherichia coli. Biochem. J.* **317,** 891–899

27. Kitamura, A., Sengoku, T., Nishimoto, M., Yokoyama, S., and Bessho, Y. (2011) Crystal structure of the bifunctional tRNA modification enzyme MnmC from *Escherichia coli. Protein Sci.* **20,** 1105–1113

28. Terwilliger, T. (2004) SOLVE and RESOLVE. Automated structure solution, density modification, and model building. *J. Synchrotron Radiat.* **11,** 49–52

29. Emsley, P., Lohkamp, B., Scott, W. G., and Cowtan, K. (2010) Features and development of Coot. *Acta Crystallogr. D Biol. Crystallogr.* **66,** 486–501

30. Collaborative Computational Project No. 4 (1994) The CCP4 suite. Programs for protein crystallography. *Acta Crystallogr. D. Biol. Crystallogr.* **50,** 760–763

31. Laskowski, R. A., MacArthur, M. W., Moss, D. S., and Thornton, J. M. (1993) PROCHECK. A program to check the stereochemical quality of protein structures. *J. Appl. Crystallogr.* **26,** 283–291

32. Gehrke, C. W., Kuo, K. C., McCune, R. A., Gerhardt, K. O., and Agris, P. F. (1982) Quantitative enzymatic hydrolysis of tRNAs. Reversed-phase high-performance liquid chromatography of tRNA nucleosides. *J. Chromatogr.* **230,** 297–308

33. Gehrke, C. W., and Kuo, K. C. (1989) Ribonucleoside analysis by reversed-phase high-performance liquid chromatography. *J. Chromatogr.* **471,** 3–36

34. Schubert, H. L., Blumenthal, R. M., and Cheng, X. (2003) Many paths to methyltransfer. A chronicle of convergence. *Trends Biochem. Sci.* **28,** 329–335

35. Barbe, V., Cruveiller, S., Kunst, F., Lenoble, P., Meurice, G., Sekowska, A., Vallenet, D., Wang, T., Moszer, I., Médigue, C., and Danchin, A. (2009) From a consortium sequence to a unified sequence. The *Bacillus subtilis* 168 reference genome a decade later. *Microbiology* **155,** 1758–1775

36. Chen, P., Crain, P. F., Näsvall, S. J., Pomerantz, S. C., and Björk, G. R. (2005) A "gain of function" mutation in a protein mediates production of novel modified nucleosides. *EMBO J.* **24,** 1842–1851

37. Watanabe, K., Oshima, T., Saneyoshi, M., and Nishimura, S. (1974) Replacement of ribothymidine by 5-methyl-2-thiouridine in sequence GT psi C in tRNA of an extreme thermophile. *FEBS Lett.* **43,** 59–63

38. Kowalak, J. A., Dalluge, J. J., McCloskey, J. A., and Stetter, K. O. (1994) The role of post-transcriptional modification in stabilization of transfer RNA from hyperthermophiles. *Biochemistry* **33,** 7869–7876

39. Shigi, N., Sakaguchi, Y., Suzuki, T., and Watanabe, K. (2006) Identification of two tRNA thiolation genes required for cell growth at extremely high temperatures. *J. Biol. Chem.* **281,** 14296–14306

40. de Crécy-Lagard, V., Marck, C., Brochier-Armanet, C., and Grosjean, H. (2007) Comparative RNomics and modomics in Mollicutes. Prediction of gene function and evolutionary implications. *IUBMB Life* **59,** 634–658

41. Suzuki, T., and Nagao, A. (2011) Human mitochondrial tRNAs. Biogenesis, function, structural aspects, and diseases. *Annu. Rev. Genet.* **45,** 299–329

42. Schubert, H. L., Phillips, J. D., and Hill, C. P. (2003) Structures along the catalytic pathway of PrmC/HemK, an N^5-glutamine AdoMet-dependent methyltransferase. *Biochemistry* **42,** 5592–5599

43. Newby, Z. E., Lau, E. Y., and Bruice, T. C. (2002) A theoretical examination of the factors controlling the catalytic efficiency of the DNA-(adenine-N^6)-methyltransferase from *Thermus aquaticus. Proc. Natl. Acad. Sci. U.S.A.* **99,** 7922–7927

44. Reinhart, M. P., Lewis, J. M., and Leboy, P. S. (1986) A single tRNA (guanine)-methyltransferase from *Tetrahymena* with both mono- and dimethylating activity. *Nucleic Acids Res.* **14,** 1131–1148

45. Ellis, S. R., Morales, M. J., Li, J. M., Hopper, A. K., and Martin, N. C. (1986) Isolation and characterization of the *TRM*1 locus, a gene essential for the N^2,N^2-dimethylguanosine modification of both mitochondrial and cytoplasmic tRNA in *Saccharomyces cerevisiae. J. Biol. Chem.* **261,** 9703–9709

46. Edqvist, J., Grosjean, H., and Stråby, K. B. (1992) Identity elements for N^2-dimethylation of guanosine-26 in yeast tRNAs. *Nucleic Acids Res.* **20,** 6575–6581

47. Constantinesco, F., Motorin, Y., and Grosjean, H. (1999) Characterisation and enzymatic properties of tRNA(guanine 26, N^2,N^2)-dimethyltransferase (Trm1p) from *Pyrococcus furiosus. J. Mol. Biol.* **291,** 375–392

48. Takeda, H., Hori, H., and Endo, Y. (2002) Identification of *Aquifex aeolicus* tRNA (m^{22}G26) methyltransferase gene. *Nucleic Acids Res.* Suppl. 2, 229–230

49. Ihsanawati, Nishimoto, M., Higashijima, K., Shirouzu, M., Grosjean, H., Bessho, Y., and Yokoyama, S. (2008) Crystal structure of tRNA N^2,N^2-guanosine dimethyltransferase Trm1 from *Pyrococcus horikoshii. J. Mol. Biol.* **383,** 871–884

50. Awai, T., Ochi, A., Ihsanawati, Sengoku, T., Hirata, A., Bessho, Y., Yokoyama, S., and Hori, H. (2011) Substrate tRNA recognition mechanism of a multisite-specific tRNA methyltransferase, *Aquifex aeolicus* Trm1, based on the X-ray crystal structure. *J. Biol. Chem.* **286,** 35236–35246

51. Gouet, P., Courcelle, E., Stuart, D. I., and Métoz, F. (1999) ESPript. Analysis of multiple sequence alignments in PostScript. *Bioinformatics* **15,** 305–308

52. Kleywegt, G. J. (2007) Crystallographic refinement of ligand complexes. *Acta Crystallogr. D Biol. Crystallogr.* **63,** 94–100